

Ultrasonic elastic characteristics of five kinds of metamorphic deformed coals under room temperature and pressure conditions

WANG Yun^{1*}, XU XiaoKai² & YANG DeYi³

¹ *Institute of Geochemistry, Chinese Academy of Sciences, Guiyang 550002, China;*

² *China University of Mining & Technology, College of Geoscience and Surveying Engineering, Beijing 100083, China;*

³ *Taiyuan University of Technology, Taiyuan 030024, China*

Received November 8, 2013; accepted January 23, 2014; published online July 2, 2014

The calibration of the elastic characteristics of deformed coals is essential for seismic inversion of such units, because the prediction of coal deformation is essential for both mining safety and methane production. Therefore, many samples of broken and mylonitic deformed coal were tested with ultrasonic waves in the laboratory. These samples came from four mining areas: the Huainan, Pingdingshan, Hebi and Jiaozuo coal mines, which present five different metamorphic ranks shown as cylinders striking across circular limits of steel. Under normal pressures and temperatures, ultrasonic P- and S-wave tests show that the velocities, quality factors, and elastic moduli of the deformed coals were greatly reduced compared with undeformed coals. Also, some correlation was found between the P- and S-wave velocities in the deformed coals. However, there is no evidence of linear correlations between velocity and density, velocity and quality factor, or the quality factors of P- and S-waves. Compared with the elastic characteristics of undeformed coals, such as P- and S-wave velocity ratios or Poisson's ratio, those of deformed coals generally decrease and the P-wave quality factors are less than those of S-waves. Moreover, the analysis of the relationship between pore structure and elastic modulus shows a better correlation between the P- and S-wave velocities and effective porosity, pore volume and specific surface area. Also, there are similar relationships between the pore structure and the Young's and shear moduli. However, there are no such correlations with other moduli. Correlations between these elastic moduli, pore structure, coal rank and density were not found for the various samples of deformed coals, which is consistent with only structural destruction occurring in the deformed coals with other physical properties remaining unchanged. The experimental results show that it is possible to predict the deformation of coals with multi-component seismic elastic inversion.

deformed coal, metamorphic rank, ultrasonic measurement, elastic characteristics

Citation: Wang Y, Xu X K, Yang D Y. 2014. Ultrasonic elastic characteristics of five kinds of metamorphic deformed coals under room temperature and pressure conditions. *Science China: Earth Sciences*, 57: 2208–2216, doi: 10.1007/s11430-014-4922-4

The vast majority of the coalfields in China have experienced the superposition of multiphase tectonization, leading to the development of deformed coal (Ju et al., 2005; Jiang et al., 2009; Wang et al., 2007). Because deformed coal strongly affects methods of coal mining (Zhang, 2009; Hao et al., 2000; Zhang et al., 2007) and coal-bed methane (CBM) production (Pan et al., 2011), identification of de-

formed coal becomes a major challenge in the seismic exploration of coalfields. This has become especially important as deeper coals resources are increasingly mined and as massive fracturation operations are needed during CBM production (Meng et al., 2013; Wang et al., 2011; Sun et al., 2005). For such exploration targets, precise spatial mapping of deformed coal distributions is required. Although geological and geophysical exploration techniques have improved rapidly in recent years (Zhang et al., 2005), geophysical characterization of deformed coal is not generally

*Corresponding author (email: yunwang@mail.iggcas.ac.cn)

sufficient to meet the needs of mine planning and design, coal safety or the installation of horizontal wells for CBM production (Wang et al., 2008). Qualitative geological resource mapping depends primarily on borehole and laneway information. Geophysical forecasting is applied mainly in the early prospecting stage, and generally is insufficient to meet the demands of production practice. The large-scale application of three-dimensional (3D) seismic technologies for coalfield exploration has the potential to lead to better quantitative and qualitative characterizations of deformed coal prior to coal mining, but this requires the development of new seismic exploration skills and techniques.

Improving our understanding of the elastic properties (e.g., velocity) of deformed coal is one of the first steps needed for the seismic exploration of deformed coal. The elastic properties of such deformed coals have been the subject of recent research (Lü, 1995; Guo et al., 1998; He et al., 1999; Peng et al., 2004; Zhang et al., 2006; Peng et al., 2008; Yao et al., 2011). Some progress has been made in the detection of deformed coal using laneway and ground-based seismic methods (Tang et al., 2002; Peng et al., 2005; Sun et al., 2011; Lu et al., 2011). However, it is very difficult to sample and prepare standard laboratory samples of deformed coal, since its structure is often loose, and its elasticity is seldom tested. Therefore, current knowledge of the elastic parameters of deformed coal, which is limited to a few mining areas and coal types, is scarce or experimental. Because of the lack of rigorous physical experiments, forecasts of the spatial distribution of deformed coal using the joint inversion of seismic data and logging data are poorly constrained (Chen et al., 2010; Chen et al., 2009). For example, He et al. (1999) used ultrasonic wave to test coals of different structures on samples sourced mainly from Pingdingshan coal mine in Henan Province, but the metamorphic degrees of the coals were similar. A broader knowledge of the elastic properties was not possible because only the P-wave velocity was measured. Guo et al. (1998) modeled deformed coal using die-cast molding with deformed coal powder of different particle sizes under a pressure of 6 MPa. These results showed that the P-wave velocity of deformed coal increases with confining pressure; as the degree of structural damage increases, the velocity becomes reduced; also, the P-wave velocity shows anisotropy (commonly 5%–10%). Because the original coal structure and state were destroyed after die-cast molding, it is difficult to evaluate their similarity and comparability by comparing samples with coals produced under geological conditions. Therefore, the experimental results only have a certain reference value. Using well log data, Peng et al. (2004) carried out statistical analyses of the density and P-wave velocity differences between deformed and undeformed coal in the Huainan coalfield. Because coal seams are soft relative to other sedimentary rocks in the region, diameter expansion and collapse of the drilling holes would have unpredictable influences on the measurement and interpretation of the data.

Therefore, there are many uncertainties in elastic properties that are determined using logging curves; also, such determinations are regionally limited to the deformed coal in Huainan.

In conclusion, because determinations of elastic properties of deformed coal are limited to a few samples and drillings from a limited number of coal mines and fields, our understanding of the elastic properties of such units with varying degrees of metamorphic change and damage is extremely limited. Therefore, the development of a better understanding of the elastic moduli of deformed coals with different degrees of metamorphic change and damage is urgent and necessary. The use of ultrasonic measurements is just one way to implement a scheme of seismic exploration for deformed coal.

1 Test samples and methods

Coal is a soft sedimentary rock that is found in seams with a lot of structural interfaces such as bedding, cleats and cracks. There are two main problems in the ultrasonic measurement of deformed coal.

(1) Deformed coal has been damaged by tectonic stress and generally has become so loose in structure that it is easily broken. It is difficult to collect clumping samples down a hole. However, extrusion molds of broken deformed coal can be measured in the lab. So, there is a great difference in elastic moduli of molded samples and those that formed under in situ geological conditions.

(2) Because transmitted S-wave arrivals will be overlapped by other wave modes during ultrasonic measurement of shear waves, the accurate calculation of S-wave velocity is difficult. This will cause a greater error in the calculation of the shear wave quality factor (Q_s).

1.1 Deformed coal sample preparation

To address the first question, the following sampling method is undertaken. First, a machined cylindrical mold is beaten directly into the deformed coal seam, and then the sample is removed while preserving its original state. Second, a suitable amount of adhesive is added to the two head faces of the cylindrical mold to make them as firm as possible. Finally, sandpaper is used to polish the two faces to facilitate coupling between the faces and transducers in the measurements followed. Some of the experimental deformed coal samples are shown in Figure 1. Apparently, adhesive can change the original structure of the deformed coal and cause the measured travel-time of the ultrasonic signal to decrease. However, because of the large scale of the samples (Table 1), the impacts of this structural change over such a short distance at ultrasonic speeds can be ignored. The measured ultrasonic time difference therefore should objectively reflect the original structure of the



Figure 1 Deformed coal samples used for testing.

deformed coal.

1.2 Ultrasonic measurements for deformed coal and data collection

To address the second question, two methods have been tried. First, observations of shear waves are made in two orthogonal directions. Based on the polarization differences among various types of body waves, the method proposed by Zhang et al. (2013) was used to pick the first arrivals of S-waves and improve S-wave recognition. Second, appropriate filters were designed to improve the calculation precision of shear wave velocity and quality factor measurements based on the frequency difference between P- and S-waves.

The equipment and technologies used for this ultrasonic experiment on deformed coal have been presented previously (Wang et al., 2012, 2013). P- and S-wave frequencies were both set to 100 kHz for the tests. Overall, the measurement system error is less than 1%. However, because of the complexity and extreme difficulty of sample preparation and measurement, the system testing error is deemed to have been controlled within 3%.

Specific test conditions are as follows.

(1) Selection of low frequency probe. Taking the sample size into consideration (6 cm in diameter and 6 cm in

height), and to avoid the attenuation of high frequency waves, 100 kHz low frequency ultrasonic probes were selected.

(2) Controlled water saturation. The primitive moisture (including free water, bound water and water of crystallization) of these samples was inevitably damaged when it was removed from the coal seam. Because coal elasticity is affected by moisture to some extent, the influence of the state of the reservoir water and its saturation on the elasticity was not considered in the experiment. Consistent moisture conditions were ensured by exposing samples to natural air conditions for a period of time (7 days in this experiment), then soaking in water for 24 h, and drying in the air for 5 h more.

(3) Load plan. To maintain the consistency of test conditions for the different laboratory samples, a clamp holder was used to attach the probes to both ends of the coal sample at the same pressure, in case of poor coupling. The pressure imposed on the holders was set to 10 kPa, the lowest hardness expected for coal samples.

1.3 Sample information

The deformed coal samples were collected from four different mining areas and classified into five different metamorphic grades. During the sampling process, the steel mold was driven into the working face in the strike direction of the coal seam. Therefore, the sample axial direction—the X direction—is defined by the labeling method used by Wang et al. (2012). During sample collection, the occurrence states of these deformed coals were compiled (Table 1).

2 Experimental results and analysis

2.1 Measurement and conversion results

All V_p (P-wave velocity), V_s (S-wave velocity), elastic modulus and quality factor data were collected and calculated from the transmitted waveform in ultrasonic measurements according to accepted elastic modulus calculation methods (Wang et al., 2013; Cheng, 2012). These data are presented in Tables 2 and 3.

Table 1 Test sample information^{a)}

Coal sample No.	Metamorphic grade	Sampling mines	Coal seam	Specific sampling points	Sample processing specification	Sample quantity (piece)	Coal industry analysis		
							M_{ad} (%)	A_d (%)	V_{daf} (%)
1	Gas coal	Huainan Panyi mine	13-1 Shihezi Group	2331(3) working face 30 m	Cylinder of 6 cm in diameter and 6 cm in height	4	1.82	12.21	37.01
2	Fat coal	Pingdingshan 8th mine	Wu9-10 Shihezi Group	12160 working face 177 m	Same as above	5	1.67	30.54	33.34
3	Coking coal	Pingdingshan 8th mine	Ji15 Shanxi Group	14120 working face 22.5 m	Same as above	5	1.58	7.03	22.56
4	Meager-lean coal	Hebi 6th mine	2-1 Shanxi Group	2143 working face 50 m	Same as above	6	1.48	8.30	13.48
5	Anthracite coal	Jiaozuo Guhanshan mine	2-1 Shanxi Group	14181 working face 75 m	Same as above	5	2.85	10.99	7.71

a) M_{ad} , Water mass fraction of experimental coal samples; A_d , ash mass fraction of air-dry base; V_{daf} , volatiles mass fraction of dry and ash-free base. Industrial analyses were carried out according to GB/T212-2001, China standard.

Table 2 Calculated V_P , Q_P , V_S , Q_x and Q_y ^{a)}

Coal sample No.	Block No.	V_P (m s ⁻¹)	Q_P	V_S (m s ⁻¹)	Q_S		ρ (g cm ⁻³)
					Q_x	Q_y	
1	1-1	857	1.03	545	1.50	1.26	1.28
	1-2	667	0.94	400	1.78	1.82	1.27
	1-3	857	1.02	545	1.37	1.65	1.22
	1-4	938	0.74	566	1.77	1.49	1.17
2	2-1	706	0.59	368	1.07	1.52	1.28
	2-2	522	0.92	324	0.83	0.89	1.25
	2-3	833	0.28	455	0.65	1.09	1.27
	2-4	759	0.69	508	0.86	0.71	1.29
	2-5	789	0.40	522	1.10	1.08	1.28
3	3-1	583	0.60	400	0.46	0.62	1.31
	3-2	750	0.37	400	0.23	0.36	1.33
	3-3	698	0.40	357	1.40	1.02	1.35
	3-4	732	0.38	423	1.31	0.98	1.38
	3-5	632	0.54	324	0.75	1.52	1.35
4	4-1	759	0.48	429	0.46	0.31	1.40
	4-2	706	0.47	429	0.46	1.26	1.41
	4-3	706	0.55	375	0.4	0.47	1.39
	4-4	674	0.49	400	0.50	0.43	1.43
	4-5	600	0.57	400	0.48	0.91	1.37
	4-6	714	0.41	286	0.15	0.78	1.41
5	5-1	741	0.39	462	1.17	2.40	1.51
	5-2	870	0.88	400	0.37	0.54	1.53
	5-3	698	0.28	451	0.32	0.89	1.47
	5-4	638	0.58	420	1.16	1.14	1.52
	5-5	870	0.30	500	0.82	0.57	1.51

a) Q_P , P-wave quality factor; Q_S , S-wave quality factor; Q_x and Q_y , the two shear-wave quality factors in orthogonal polarization directions; ARD or ρ , apparent density.

Table 3 Calculated results for five mechanical elastic parameters^{a)}

Coal sample No.	Block No.	λ (GPa)	μ (GPa)	ν	K (GPa)	E (GPa)
1	1-1	0.18	0.38	0.16	0.43	0.88
	1-2	0.16	0.20	0.22	0.29	0.50
	1-3	0.17	0.36	0.16	0.41	0.84
	1-4	0.28	0.37	0.21	0.53	0.91
2	2-1	0.29	0.17	0.31	0.41	0.46
	2-2	0.08	0.13	0.19	0.17	0.31
	2-3	0.36	0.26	0.29	0.53	0.68
	2-4	0.08	0.33	0.09	0.30	0.73
	2-5	0.10	0.35	0.11	0.33	0.77
3	3-1	0.03	0.21	0.06	0.17	0.44
	3-2	0.32	0.21	0.30	0.46	0.55
	3-3	0.31	0.17	0.32	0.43	0.46
	3-4	0.25	0.25	0.25	0.41	0.62
	3-5	0.26	0.14	0.32	0.35	0.37
4	4-1	0.29	0.26	0.27	0.46	0.65
	4-2	0.18	0.26	0.21	0.36	0.63
	4-3	0.30	0.20	0.30	0.43	0.51
	4-4	0.19	0.23	0.23	0.34	0.56
	4-5	0.05	0.22	0.10	0.20	0.48
	4-6	0.49	0.12	0.40	0.57	0.32
5	5-1	0.18	0.32	0.18	0.40	0.76
	5-2	0.67	0.24	0.37	0.83	0.67
	5-3	0.12	0.30	0.14	0.32	0.68
	5-4	0.08	0.27	0.12	0.26	0.60
	5-5	0.39	0.38	0.25	0.64	0.95

a) λ , Lamé constant; μ , shear modulus; ν , Poisson's ratio; K , bulk modulus; E , Young's modulus.

2.2 Elastic characteristics

From Table 2, the following viewpoints can be raised. First, note that the average V_P (737 m s⁻¹), V_S (433 m s⁻¹) and V_P/V_S (1.702) of the deformed coal are far less than those of undeformed coal (Wang et al., 2012). The correlation between V_P or V_S and density is very poor. Density differences between undeformed and deformed coal are not obvious, so structural differences can have significant effects on the speed of the traveling wave. The V_P and V_S of deformed coal are obviously different, and can be linearly separated from those of undeformed coals since their V_P and V_S values are less than 1000 m s⁻¹. As mentioned, the samples can be divided into five categories based on metamorphic degree, which means that we can define five groups of V_P and V_S values. Through the linear regression analysis of V_P and V_S shown in Figures 2 and 3, a good linear correlation between the mean V_P and V_S of each group can be made. These linear correlations vary significantly. The maximum vitrinite reflectivity (Table 4) and analysis of the relationship between density and velocity (Table 2) show that there is a certain correlation between density and degree of metamorphism. However, there is no correlation between the five groups of mean V_P and V_S values and metamorphic grade.

To synthetically illustrate the characteristics of Q_P and

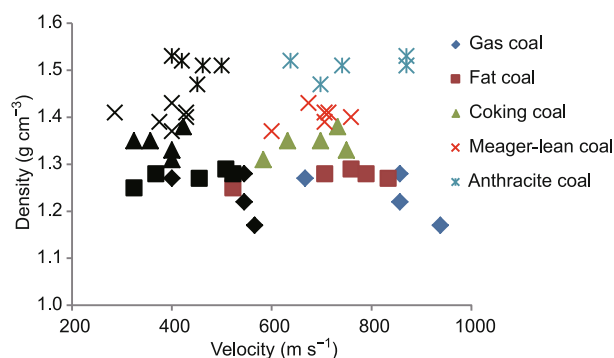


Figure 2 Velocity versus density. The color symbol represents the P-wave velocity and the black S-wave's.

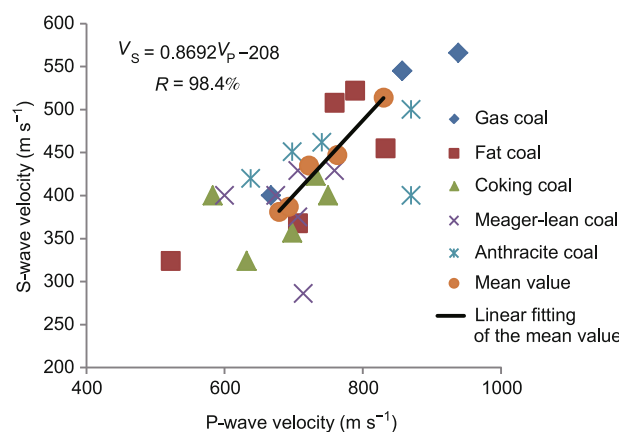


Figure 3 Relationships between V_P and V_S .

Table 4 Pore structure determination results^{a)}

Coal sample No.	Metamorphic grade	Total pore volume (cm ³ g ⁻¹)	Average pore diameter (nm)	Effective porosity (%)	R _{o,max} (%)	BET specific surface area (m ² g ⁻¹)	Deformed coal types
2	Fat coal	0.01996	8.118	2.54	1.346	9.836	Broken particle coal
3	Coking coal	0.003213	4.588	0.43	1.494	2.801	Mylonitic coal
4	Meager-lean coal	0.004559	7.343	0.64	1.672	3.462	Mylonitic coal
5	Anthracite coal	0.02508	6.660	3.78	2.548	15.06	Mylonitic coal

a) R_{o,max}, Maximum vitrinite reflectance. Effective porosity is calculated with the total pore volume and the apparent relative density (Zhang, 2009).

Q_s, the mean value of the quality factors in the two orthogonal directions is treated as the quality factor in the direction of wave propagation direction (Figure 4). From Table 2 and Figure 4, we see that the quality factors of deformed coal are generally low (<2). Q_p is nearly half of Q_s for most of the samples. There is no correlation between Q and speed, therefore there is no physical basis for estimating quality factor based on speed. However, from the relationship between Q_p and Q_s (Figure 5), some conclusions can be drawn. Although Q_s generally gets larger as Q_p increases, there is no linear correlation between Q_p and Q_s. Also, there is no

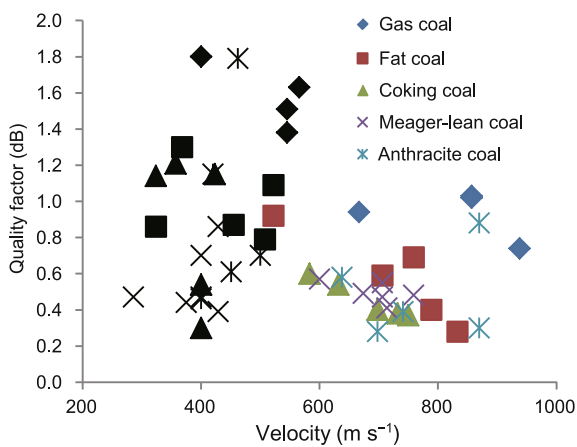


Figure 4 Relationships between velocity and Q. The color symbol represents Q_p and the black Q_s.

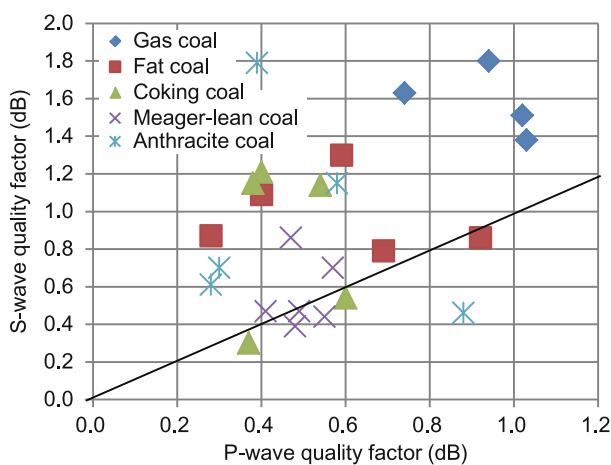


Figure 5 Relationships between Q_p and Q_s.

correlation between Q and metamorphic grade, which is unlike the situation with general sedimentary rocks and undeformed coal (Wang et al., 2013, 2009). According to the bisectrix in Figure 5, Q_s is generally greater than Q_p. Therefore, the absorption and attenuation effects of deformed coal for P-waves are much stronger, which has significance for the recognition of deformed coal with multiple waves.

Some results can be found by contrasting Q_x and Q_y (Table 2). If $2|(Q_x - Q_y)/(Q_x + Q_y)|$ is regarded as the anisotropy coefficient, then the variability of Q_s anisotropy is found to be intense, ranging from 1.7% to 135%, but predominantly from 30% to 40% with a coefficient average of 38.5%. The destructive effect of tectonic stress is deduced to cause greater azimuthal differences in Q_s for a given coal seam, even though the anisotropy coefficient is independent of the metamorphic degree.

The elastic modulus values (Table 3) show that, with the exception of Poisson's ratio, the elastic moduli of the deformed coals are small (Wang et al., 2013), and less than 1 GPa. This shows that the resistance strength of the deformed coal to crushing and shearing deformation is very low, and that it is partially kept in a state of stress equilibrium by the surrounding rocks in the coal seam. However, if this balance is disequilibrated, it is difficult for the deformed coal to bear the high ground stress. This is one of the reasons why the detection of deformed coal is of great importance for deep coal mining and gas extraction.

2.3 Relationship between pore structure and elastic moduli in deformed coal

Because deformed coal is generally implicated in the formation of a dynamic disaster within a coal mine, and is generally avoided during horizontal fracturing operations, an evaluation of its pore structure is meaningful (Cheng, 2012; Ju et al., 2004). In particular, deformed coal may adsorb excessive gas. The pore volume and specific surface area are two important indicators for weighing the absorption capacity of deformed coal (Hou et al., 2012; Ju et al., 2005). Pore volume and effective porosity, which provide an indication of the pore structure, are the two main indicators of the gas desorption and diffusion rate in CBM production (Chen et al., 2010). Therefore, the specific surface area and pore structure of samples were measured (Table 4).

N_2 absorption and Hg injection were undertaken as part of the determination of the pore structure, for which N_2 adsorption is mainly used to determine the pore size distribution (<50 nm) in the coal, and the Hg injection experiment is mainly used to determine the pore size distribution (>50 nm) of mesopores and macropores in the coal. Vitrinite reflectance was analyzed in China according to GB/T6948-2008 and the specific surface areas were measured with N_2 absorption according to GB/T7702.20-2008.

Note the following differences. Gas coal samples from Huainan coalfield were used in the ultrasonic measurements, but gas coal samples from Henan coalfield were used for pore structure measurements. Because of this regional difference, gas coal was not considered in the following analyses of the relationship between pore structure and elastic moduli.

Because the density was almost unchanged during the deformation of the deformed coal, while the pore structure changed greatly, there are no obvious correlations between the total pore volume, average pore diameter, effective porosity and density. However, as seen by comparing and contrasting Tables 2 and 4 (Figure 6), there are good correlations between V_p , V_s and total pore volume, effective porosity and specific surface area, even though there are no correlations between V_p , V_s and average pore diameter. Because of the non-quantitative characteristics used to classify coal body structure, it is difficult to determine a relationship between the degree of damage to coal structure and the pore structure (Table 4). In practice, pore volume and the specific surface area should increase according to the degree of damage of the deformed coal and also because of the increase based on the classification method (Ju et al., 2005) and microstructural analysis. Therefore, a simple classification of three types of deformed coal shows finite precision in reflecting microstructure.

After a comprehensive analysis of Tables 3 and 4, we can investigate the relationship between the elastic moduli and pore structure (Figure 7). It is apparent that the correlations between Young's modulus, shear modulus, specific surface area and the effective porosity are better. This improved correlation coincides with the relationship between velocities and pore structure caused by the conversion relationship within the velocities and elastic moduli.

Through the pore structure data (Table 4), the total pore volume, effective porosity and BET specific surface area increase with metamorphic degree, which increases from coking coal to anthracite coal, consistent with the relationship of metamorphic degree to density. There are positive correlations between velocities, moduli and the degree of development of pore structure. In fact, the influence of pore structure on the velocities and moduli is embodied in their macro-density influence on velocities and moduli. However, when fat coal with a low metamorphic grade and a low density is considered, its total pore volume, effective porosity and BET specific surface area are significantly

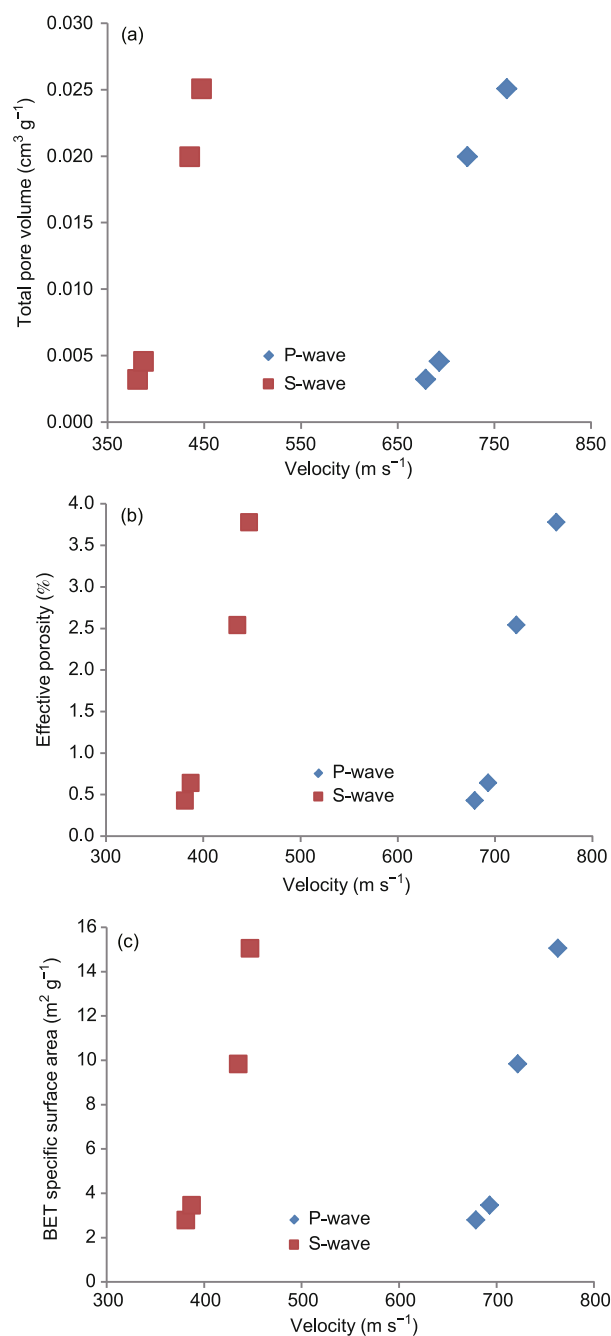


Figure 6 The relationship between velocities and pore structure. (a) The relationship between velocities and total pore volume; (b) the relationship between velocities and effective porosity; (c) the relationship between velocities and BET specific surface area.

higher than those of coking coal and meager-to-lean coal, but only slightly less than those of anthracite, which reflects the limitation of the above law. The average pore size of the fat coal is maximized and the fat coal samples belong to a broken particle of coal (others belong to mylonitic coal). The fundamental difference in the pore-fracture structure is that the influence of the fat coal on velocities and moduli is very different from the influences of other coals.

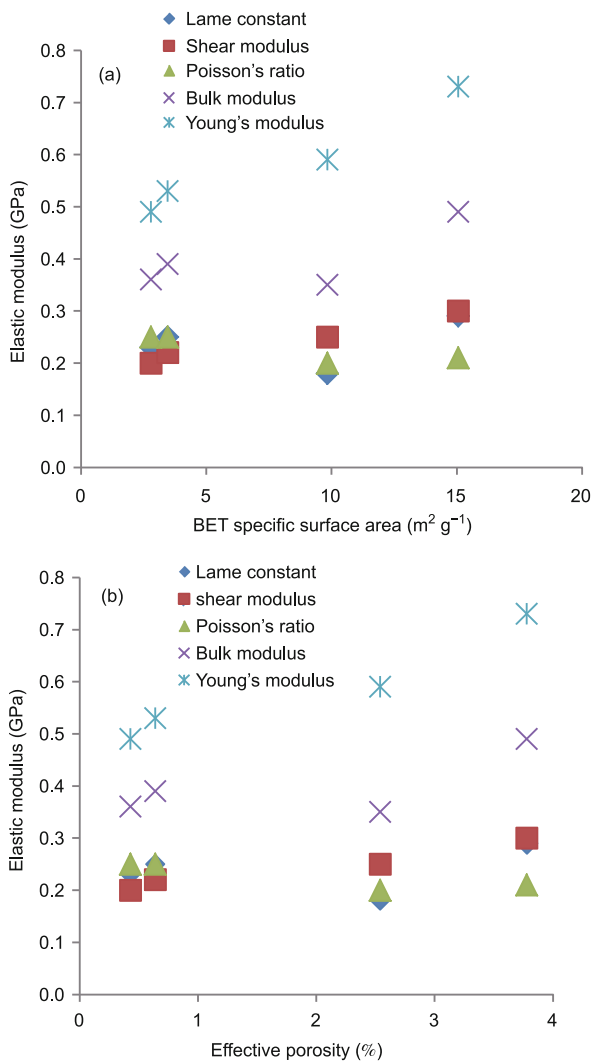


Figure 7 Relationship between elastic moduli and pore structure. Poisson's ratio unit is 1. (a) The relationship between elastic moduli and BET specific surface area; (b) the relationship between elastic moduli and effective porosity.

3 Discussion

Because regions of deformed coal restrict CBM production and coal mining, the need for elastic measurements of deformed coal is urgent so that a basic physical support can be provided for seismic characterizations in such settings. In this paper, deformed coal samples extracted from four different mining areas and characterized by five different metamorphic grades (medium to high) and two degrees of structure damage were evaluated in the laboratory with ultrasonic transmissions.

Because the physical composition and structure of coal are extremely complex topics, the measured ultrasonic wave velocities must be a comprehensive reflection of geological parameters such as material composition, pore structure and bedding structure. Therefore, after merging multiple test results for the coal samples, an analysis of the results can

provide some control on the general characteristics of the coal. Mean values calculated from Table 2 are shown in Table 5. The most important conclusion is the observation that the V_P and V_S of the deformed coal decrease with good correlation between each other. There are poor linear correlations between V_P , V_S and density. The results of regression analysis between mean V_P , V_S and mean density are shown in Figure 8. There are stronger quadratic correlations between mean V_P , V_S and mean density. With an increase of density, V_P and V_S first decrease and then increase on the whole. The correlations between average density and the industrial analysis index for each coal are analyzed in the same way. There are stronger quadratic correlations between M_{ad} (moisture), V_{daf} (volatiles) and density. However, there is no correlation between ash content and density. Because a uniform treatment of moisture was undertaken for samples prior to testing, the influence of moisture is not considered in the analysis. Sample density is mainly influenced by metamorphic grade, which indirectly affects the elastic response characteristics. The before-mentioned influence of pore structure on elastic parameters should be the concrete manifestation of the influence of macroscopic structural damage on the elastic responses. The ratio of V_P and V_S for deformed coal is 1.7:1, which is lower than that of undeformed coal.

The second conclusion is that Q_P and Q_S are very small. This means that the absorption effect of the elastic waves in deformed coal is strong, which is in agreement with its characteristic low strength. There are poor correlations

Table 5 Mean values of ρ , V_P and V_S

Coal sample No.	ρ (g cm ⁻³)	V_P (m s ⁻¹)	V_S (m s ⁻¹)
1	1.24	830	514
2	1.27	722	435
3	1.34	679	381
4	1.40	693	387
5	1.51	763	447

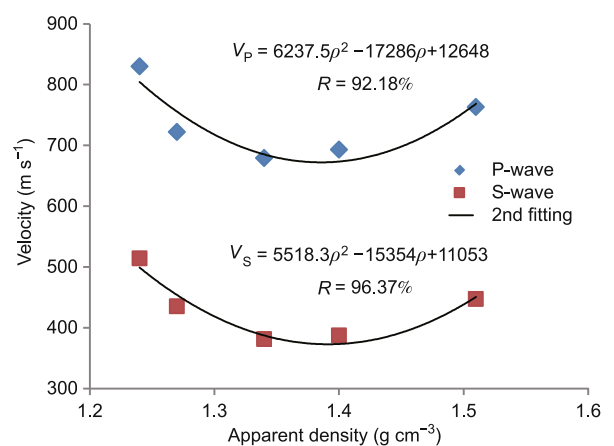


Figure 8 Correlations between the mean V_P , V_S and ρ .

Table 6 Pore structure comparisons between deformed and undeformed coal

Coal sample No.	Metamorphic grade	Total pore volume ($\text{cm}^3 \text{g}^{-1}$)		Average pore diameter (nm)		Effective porosity (%)	
		Undeformed coal	Deformed coal	Undeformed coal	Deformed coal	Undeformed coal	Deformed coal
2	Fat coal	0.00972	0.01996	5.474	8.118	1.39	2.54
3	Coking coal	0.005716	0.003213	4.037	4.588	0.83	0.43
4	Meager-lean coal	0.008957	0.004559	5.195	7.343	1.25	0.64
5	Anthracite coal	0.005208	0.02508	3.953	6.660	0.85	3.78

between quality factors and wave velocities. The same characteristics exist between Q_P and Q_S , with an average anisotropic coefficient of Q_S of 38%.

Table 6 compares the pore structures of deformed and undeformed coal. The average pore size of deformed coal is generally greater than that of the corresponding undeformed coal. This may be the main reason why the attenuation of elastic waves in deformed coal is greater than in the corresponding undeformed coal.

By comparing corresponding test results of deformed and undeformed coal (Wang et al., 2012, 2013; Cheng, 2012), the velocities, Q values, speed ratios and elastic moduli of deformed coal are observed to reduce significantly as a result of changes in coal body structure from matrix-fissure to broken and mylonitic particles. The above analysis provides basic experimental support for the detection of deformed coal by using further elastic inversion with effective rock physics support.

Now, because there is no unified standard for the classification of deformed coal damage in geology (e.g., Ju et al., 2005; Zhang, 2009), the classification of coal structure damage is based on qualitative analyses of coal samples. The deformed coal is divided into two simple categories in the field sampling and laboratory observations presented in this paper. Due to an absence of quantitative description parameters for the qualitative analysis and definition of structural damage, elastic characteristic differences found in the various kinds of damaged coal are not discussed in this paper. The formation of precise and quantitative microscopic descriptions of deformed coals is required to predict the degree of damage in deformed coal using seismic exploration techniques. To make use of basic ultrasonic experimental results in practical seismic exploration, the transition from ultrasonic waves to lower-frequency seismic waves must be considered, since there can be a significant difference in elastic parameters at different frequencies (i.e., those used in laboratory ultrasound studies and those used in field-based seismic experiments). Because ultrasonic measurement is implemented under normal pressure and temperature conditions, the results of this paper only provide a relative guide for simulating actual formation conditions.

According to experimental ultrasound results (Zhou et al., 2012) conducted under different temperature and pressure conditions for coal samples with both developed and undeveloped cleats, and in view of the temperature conditions

needed for the development of China's current coal and CBM resources, temperature is found to have little effect on the speed of coal with different cleat developments. For example, velocities could increase by nearly 10% with an increase in pressure for coal samples with cleat development, but only increase by < 5% for coal samples with undeveloped cleats. Although the results of the tests presented in this paper were achieved under normal temperature and pressure conditions, it is still possible to compare physical characteristics such as velocities, elastic moduli and the relationships between these properties and density under both experimental and field conditions. This provides a significant reference for the seismic detection of deformed coal.

This work was supported by National Natural Science Foundation of China (Grant Nos. 41172145, 41372163 and 41104084), National Basic Research Program of China (Grant No. 2014CB440905), National Special Fund of China (Grant Nos. 2011ZX05: 035-001-006HZ and 035-002-003HZ, 008-006-22, 049-01-02 and 019-003), and PetroChina Innovation Foundation (Grant No. 2011D-5006-0303). Prof. Wei Jianxin, of China University of Petroleum (Beijing) is thanked for providing technical support for the ultrasound measurements. Thanks should also be given to Professor Zhang Yugui, Institute of Gas Geology in Henan Polytechnic University for guidance in the industrial coal analysis and determination of pore structure. Shen Zhenhua and Cheng Lin have undertaken some sample preparations and laboratory measurements.

- Chen F Y, Ju Y W, Li X S, et al. 2010. Diffusion-osmosis characteristics of coalbed methane in tectonically deformed coals and their mechanism (in Chinese). *Earth Sci Front*, 17: 195–201
- Chen T J, Wang X, Cui R F. 2010. The detectability analysis on HTI tectonic coal cracks by azimuthal AVO's forward modeling (in Chinese). *J Chin Coal Soc*, 35: 640–644
- Chen T J, Cui R F, Liu E R. 2009. AVO forward modeling for VTI coal (in Chinese). *J Chin Coal Soc*, 34: 438–442
- Cheng L. 2012. Research on geophysical response of deformed coal (in Chinese). Master Dissertation. Jiaozuo: Henan Polytechnic University
- Guo D Y, Han D X, Feng Z L. 1998. Experimental research on wave velocity of deformed coal characteristics under the ambient pressure (in Chinese). *Coal Sci Technol*, 26: 21–24
- Hao J S, Yuan C F, Zhang Z X. 2000. The tectonic coal and its effects on coal and gas outburst (in Chinese). *J Jiaozuo Inst Technol (Nat Sci)*, 19: 403–406
- He J S, Lü S L. 1999. Gas Outburst Geophysical Research (in Chinese). Beijing: Coal Industry Press
- Hou Q L, Li H J, Fan J J, et al. 2012. Structure and coalbed methane occurrence in tectonically deformed coals. *Sci China Earth Sci*, 55: 1755–1763
- Jiang B, Qin Y, Ju Y W et al. 2009. The coupling mechanism of the evolution of chemical structure with the characteristics of gas of tectonic coals (in Chinese). *Earth Sci Front*, 16: 262–271
- Ju Y W, Jiang B. 2005. Tectonic Coal Structure and Reservoir Physical

- Property (in Chinese). Xuzhou: China University of Mining and Technology Press
- Ju Y W, Jiang B, Hou Q L, et al. 2004. The new structure-genetic classification system in tectonically deformed coals and its geological significance (in Chinese). *J Chin Coal Soc*, 29: 513–517
- Ju Y W, Jiang B, Hou Q L, et al. 2005. The relationship of nanoscale deformation in coal structure and metamorphic deformation environment (in Chinese). *Chin Sci Bull*, 50: 1884–1892
- Lu J, Wang Y, Shi Y. 2011. Coal hardness prediction using joint inversion of multi-wave seismic data and logging (in Chinese). *Chin J Geophys*, 54: 2967–2972
- Lü S L. 1995. The theoretical basis of forecasting coal body structure with hole ultrasonic gauge (in Chinese). *J Jiaozuo Mining Inst*, 14: 54–58
- Meng Z P, Hou Q L. 2013. Coupling model of stress dependent permeability in high rank coal reservoir and its control mechanism (in Chinese). *Chin J Geophys*, 56: 667–675
- Pan Z J, Luke D. Connell. 2011. Modelling of anisotropic coal swelling and its impact on permeability behaviour for primary and enhanced coalbed methane recovery. *Int J Coal Geol*, 85: 257–267
- Peng S P, Du W F, Yuan C F, et al. 2008. Identification and forecasting of different structural coals by P-wave and S-wave from well-logging (in Chinese). *Acta Geol Sin*, 82: 1311–1322
- Peng S P, Gao Y F, Peng X B, et al. 2004. Study on the rock physic parameters of coal bearing strata Huainan coal field (in Chinese). *J Chin Coal Soc*, 29: 177–181
- Peng S P, Gao Y F, Yang R Z, et al. 2005. Theory and application of AVO for detection of coalbed methane (in Chinese). *Chin J Geophys*, 48: 1475–1486
- Sun X K, Cui R F, Mao X R, et al. 2011. Elastic impedance inversion associated with simultaneous inversion in determining the distribution of tectonic coal (in Chinese). *J Chin Coal Soc*, 36: 778–783
- Sun X M, He M C. 2005. Numerical simulation research on coupling support theory of laneway within soft rock at depth (in Chinese). *J Chin Univ Mining Technol*, 34: 166–169
- Tang Y Y, Chen J F, Peng L S. 2002. Study of tectonic coal by radio-wave pit perspective (in Chinese). *J Chin Coal Soc*, 27: 254–258
- Wang E Y, Yin Q C, Li F L. 2008. Research state and its development trends of structure coal (in Chinese). *J Henan Polytech Univ (Nat Sci)*, 127: 278–281
- Wang H M, Zhu Y M, Li W, et al. 2011. Two major geological control factors of occurrence characteristics of CBM (in Chinese). *J Chin Coal Soc*, 36: 1129–1134
- Wang Y, Lu J, Shi Y, et al. 2009. *PS*-wave *Q* estimation based on the *P*-wave *Q* values. *J Geophys Eng*, 6: 386–389
- Wang Y, Xu X K, Zhang Y G. 2012. Characteristics of *P*- and *S*-wave velocities and their relationships with density of six metamorphic kinds of coals (in Chinese). *Chin J Geophys*, 55: 3754–3761
- Wang Y, Zhang Y G, Xu X K. 2013. Relations between the maximum vitrinite reflectance and the elastic parameters of six metamorphic kinds of coals (in Chinese). *Chin J Geophys*, 56: 2116–2122
- Wang Z R, Chen L X, Cheng C R et al. 2007. Forecast of geological gas hazards for “Three-Soft” coal seams in gliding structural areas. *J Chin Univ Mining Technol*, 17: 484–488
- Wu X Y. 2000. Study on acoustic wave and related property in petroleum fluid (in Chinese). Doctoral Dissertation. Beijing: Institute of Geology and Geophysics, Chinese Academy of Sciences
- Yao J P, Sima L Q, Zhang Y G. 2011. Quantitative identification of deformed coals by geophysical logging (in Chinese). *J Chin Coal Soc*, 36: 94–98
- Zhang J L, Wang Y, Zhang Y G. 2013. Application of shear wave polarization method in ultrasonic measurement of coal samples (in Chinese). *J Chin Coal Soc*, 38: 1220–1226
- Zhang S H, Peng S P, Liu Y X. 2006. Experimental study on properties of acoustic velocity in crack rocks of coal-bearing strata (in Chinese). *J Shandong Univ Sci Technol (Nat Sci)*, 25: 28–31
- Zhang Y G, Zhang Z M, Cao Y X. 2007. Deformed-coal structure and control to coal-gas outburst (in Chinese). *J Chin Coal Soc*, 32: 281–284
- Zhang Z M. 2009. Gas Geology (in Chinese). Xuzhou: China University of Mining and Technology Press. 412
- Zhang Z M, Zhang Y G. 2005. Gas Geology Rule and Gas Prediction (in Chinese). Beijing: Coal Industry Press. 126
- Zhou F, Xu M J, Ma Z G, et al. 2012. An experimental study on the correlation between the elastic wave velocity and microfractures in coal rock from the Qingshui basin. *J Geophys Eng*, 9: 691–696